Development and Characterization of Pectin-Based Antimicrobial Packaging Films Containing Nanoemulsified Trans-Cinnamaldehyde

Fatemeh Baghi, Sami Ghnimi, Géraldine Agusti, Emilie Dumas, Adem Gharsallaoui

applied sciences

MDPI

Article

Development and Characterization of Pectin-Based Antimicrobial Packaging Films Containing Nanoemulsified *Trans*-Cinnamaldehyde

Fatemeh Baghi [1,2], Sami Ghnimi [1,2,*], Géraldine Agusti [1], Emilie Dumas [1] and Adem Gharsallaoui [1,*]

[1] Laboratoire d'Automatique, de Génie des Procédés et de Génie Pharmaceutique, CNRS, University Claude Bernard Lyon 1, 43 Bd 11 Novembre 1918, 69622 Villeurbanne, France; fbaghi@isara.fr (F.B.); geraldine.agusti@univ-lyon1.fr (G.A.); emilie.dumas@univ-lyon1.fr (E.D.)

[2] ISARA, Higher Institute of Agriculture and Agri-Food Rhone-Alpes, 23 Rue Jean Baldassini, 69007 Lyon, France

* Correspondence: sghnimi@isara.fr (S.G.); adem.gharsallaoui@univ-lyon1.fr (A.G.)

Abstract: In this study, an antimicrobial plant-based film was developed using pectin which is incorporated by different percentages of nanoemulsified *trans*-cinnamaldehyde (TC). The nanoemulsion of TC was incorporated into pectin to form films containing TC at concentrations of 5.00%, 3.33%, 2.50% and 2.00% (*w*/*w*). The nanoemulsion of TC was formed by using soybean lecithin as an emulsifier and had a zeta potential of −57 mV and an average size of 106 nm. The analysis showed that the addition of emulsified TC enhanced the light barrier properties, but the opacity of films increased due to the increase in light absorption, coalescence, and light-scattering phenomena. Films containing the nanoemulsion of TC exhibited reduced tensile strength and elasticity due to structural discontinuities in the film network caused by the presence of the nanoemulsion of TC, while elongation at break increased for TC concentrations of 2.50% and 2.00%. The films retained their infrared spectra, but their thermal stability decreased slightly. The incorporation of TC nanoemulsion significantly reduced the glass transition temperature, as shown by the differential scanning calorimetry analysis. The active films showed antimicrobial activity against *Listeria innocua* and *Escherichia coli*, indicating their potential for various food applications.

Keywords: active film; *trans*-cinnamaldehyde; food packaging; nanoemulsion; antimicrobial activity

Citation: Baghi, F.; Ghnimi, S.; Agusti, G.; Dumas, E.; Gharsallaoui, A. Development and Characterization of Pectin-Based Antimicrobial Packaging Films Containing Nanoemulsified *Trans*-Cinnamaldehyde. *Appl. Sci.* **2024**, *14*, 2256. https://doi.org/10.3390/app14062256

Academic Editor: Antonio Valero

Received: 29 January 2024
Revised: 7 February 2024
Accepted: 13 February 2024
Published: 7 March 2024

1. Introduction

The preservation of food is greatly influenced by the role of food packaging, which shields it from chemical, biological, environmental, and physical harm during transportation and storage. Effective food packaging ensures the safe distribution of products to consumers in optimal conditions. In addition, microbial contamination causes food to spoil and is responsible for over 25% of food lost before it is consumed [1]. The excessive use of petroleum-based plastics has led to serious environmental problems, with annual global plastic production exceeding 350 million tons. Alarmingly, our oceans contain approximately 85% of plastic waste, posing a serious threat to the environment and human health [2]. Food packaging accounts for approximately 45% of non-biodegradable plastics [3]. In response to growing environmental concerns and the demand for natural compounds, scientists have been focused on developing biodegradable food packaging with biological activities due to their environmentally friendly properties. Biopolymer-based materials derived from plant, animal, and microbial sources have attracted attention. These materials can be enzymatically degraded by microbes [4]. Over the past two decades, extensive research has been conducted on biopolymers for food packaging applications as alternatives to petroleum-based plastics [5,6]. Biopolymer packaging materials are naturally derived from lipids, proteins, or polysaccharides [7]. Among these, polysaccharides such

as cellulose, alginate, starch, chitosan, pectin, gum, carrageenan, and pullulan have great potential for the development of food packaging [8,9]. In particular, pectin has attracted considerable attention. Pectin is a group of structurally heterogeneous polysaccharides widely distributed in the primary cell walls and middle lamella of plants. It consists of β-(1-4)-linked D-galacturonic acid with galactose and rhamnose [10]. Its structural and macromolecular properties vary depending on the used source [5]. Although apple pomace and citrus peel are the primary sources for commercial pectin production, there is an increasing demand for alternative sources to obtain pectin with different functional groups by more effectively utilizing food by-products [11,12]. Pectins have the carboxyl group of the sugar moiety in their structure, which may be partially esterified with a methyl group and partially or completely neutralized with one or more bases [13]. Based on the degree of esterification (DE), pectin can be classified to low methyl pectin (LMP) with less than 50% esterification and high methyl pectin (HMP) with more than 50% esterification [11]. The pectin properties depend on many factors, mostly including the source, extraction method, molecular weight, degree of methyl esterification, etc. [13]. Gel formation is one of the most important properties of pectin. LMP forms gel in the presence of calcium ions, which involves electrostatic interactions resulting in the formation of an eggbox model stabilized by hydrogen bonds and van der Waals interactions between the methylated groups and free carboxyl groups [14]. To prepare a pectin film-forming gel with adequate mechanical strength, rupture strength and viscosity, the molecular weight needs to be more than 300 kDa [13]. In the food industry, pectin finds various uses as a gelling agent, thickening agent, and stabilizer. Additionally, its applications extend beyond food to non-food sectors like the medical and pharmaceutical industries [11]. Due to its excellent film-forming properties, biocompatibility, biodegradability and non-toxicity, pectin is considered also an effective biopolymer for the production of film packaging [15]. Pectin-based films can be produced by different techniques such as solution casting and extrusion [16]. Because of its simplicity and the fact that it does not require special tools, solution casting is the most commonly used method on a laboratory scale [13]. The amorphous structure of pectin allows the incorporation of additives and facilitates their retention within the film structure. This property makes pectin suitable for carrying active compounds like essential oils, which could be applied to the production of active film packaging [17].

Pectin-based active packaging has great potential for food preservation applications. Some studies reported practical examples of pectin-based packaging used for food preservation. Edible pectin film containing carvacrol and cinnamaldehyde successfully inactivated *Listeria monocytogenes* on ham [18]. Reduced bacterial growth and increased oxidative stability were obtained for butter packaged with pectin-based film containing *Carum copticum* essential oils [19]. In another study, pectin film containing clove essential oil were successfully preserved beam (*Magalobrama ambycephala)* fillet in the refrigerator for 15 days [20].

Essential oils (EOs) consist of various compounds such as terpenes, aldehydes, fatty acids, phenols, ketones, esters and alcohols, have significant food preservation potential [21,22]. EOs with the ability to disrupt and penetrate the bacterial cell wall have shown interesting antimicrobial activities [23]. One important component is *trans*-cinnamaldehyde (TC), which is a major constituent of cinnamon oil. It is widely used as a flavoring agent and has agrichemical, antimicrobial, and anti-cancer properties. *trans*-cinnamaldehyde is classified as safe for use in foods by the Food and Drug Administration (FDA) [24,25]. It has antimicrobial activity against a wide range of foodborne pathogens, including both Gram-positive and Gram-negative bacteria [26,27].

Direct incorporation of EOs into water soluble biopolymer matrices such as pectin caused poor miscibility and phase separation. In addition, the free EOs in the film matrix can undergo rapid migration and lose their activity for a short time. To overcome these difficulties, the incorporation of encapsulated EOs instead of free EOs in film-forming solutions could be applied [28]. Consequently, oil-in-water nanoemulsion (NE) has been studied in various biopolymer-based active films [29–32].The use of the nanoemulsion of bioactive compounds can contribute to the improvement of pectin film properties. A

reduction in water sorption and water vapor permeability, as well as an increase in the mechanical and biological properties of pectin film incorporated with the nanoemulsion of *Origanum majorana L.* oil were reported by [28]. Pectin films containing the nanoemulsion of copaiba oil also showed a decrease in water vapor permeability and an increase in extensibility along with less stiffness, in addition to higher antimicrobial activity [33].

Therefore, this study aims to develop pectin-based films incorporating different concentrations of *trans*-cinnamaldehyde as an antimicrobial agent. The investigation will evaluate the effect of *trans*-cinnamaldehyde concentration on the physical, thermal, mechanical, and biological properties of pectin films for food packaging applications. By exploring the potential of *trans*-cinnamaldehyde-incorporated pectin films, this study contributes to the creation of eco-friendly and sustainable packaging, aiming to prolong food shelf life while mitigating plastic pollution.

2. Materials and Methods

2.1. Materials

Low methoxyl pectin (LMP) was obtained from Cargill in Baupte, France. LMP has an esterification degree ranging from 22% to 28%, an acetylation degree between 20% and 23%, and a carbohydrate content of 81.21%. Granular soybean lecithin was obtained from Acros Organics in Geel, Belguim Glycerol and trans-Cinnamaldehyde (TC) of 99% purity was acquired from Sigma-Aldrich in Steinheim, Germany. The bacteria used in this study were obtained from DSMZ-Braunschweig, German Collection of Microorganisms. Tryptone Soy Broth (TSB) and Tryptone Soy Agar plates (TSA) were purchased from Biokar Diagnostics, headquartered in Beauvais, France.

2.2. Preparation of the Nanoemulsion of Trans-Cinnamaldehyde (NE)

To prepare oil-in-water (O/W) emulsions, a mixture of 10% (*w*/*w*) *trans*-cinnamaldehyde and 2% (*w*/*w*) soybean lecithin as an emulsifier was blended via an Ultra-Turrax (IKA Werke GmbH & Co, Staufen, Germany) with distilled water operating at 15,000 rpm for 6 min. The emulsion was then subjected to two passes through a microfluidizer (Microfluidizer LM20, Microfluidics Corp, Newton, MA, USA) at a pressure of 500 bar, followed by one pass at a pressure of 1000 bar to obtain a nanoemulsion. The size distribution of the nanoemulsion was determined to confirm its particle size distribution, while the Zeta potential was measured to assess its stability.

2.3. Preparation of Films

2.3.1. Preparation of the Film-Forming Solution

To prepare film-forming solutions, pectin powder was dissolved in distilled water at a concentration of 9% and 1% (*w*/*w*) of glycerol was added and mixed until complete solubilization, which took approximately 4 h. The pectin solution was then combined with the TC nanoemulsion at 4 different ratios of pectin to TC nanoemulsion (1:1, 2:1, 3:1, 4:1) to produce the active film-forming solutions (P/NE:1, 2, 3 and 4) and mixed for a further 2 h.

2.3.2. Fabrication of Films

Films were prepared using the casting solvent method. Film-forming solutions were spread onto glass plates using an electrically driven film applicator device (Unicoater 409, ERICHZEN, Hemer, Germany) equipped with a four-way film applicator with fixed gap heights (Model 360, ERICHZEN, Hemer, Germany). The wet layer thickness was set at 1000 µm (prior to drying). Subsequently, the films were dried in an oven (UNB 400, Memmert, Büchenbach, Germany) at a temperature of 60 °C. The composition of the films prepared at different ratios is presented in Table 1. Four samples, namely P/NE:1, P/NE:2, P/NE/3, and P/NE:4, were obtained, containing 5.00%, 3.33%, 2.50%, and 2.00% (wt%) of *trans*-cinnamaldehyde, respectively.

Table 1. Composition of pectin films containing *trans*-cinnamaldehyde (TC).

Sample Names	Composition of the Film	TC Con. (% *w*/*w*)
Pectin (control)	Pectin film	0%
P/NE:1	Pectin mixed with nanoemulsion of *trans*-cinnamaldehyde at the ratio of 1:1(Pectin:NE)	5.00%
P/NE:2	Pectin mixed with nanoemulsion of *trans*-cinnamaldehyde at the ratio of 2:1 (Pectin:NE)	3.33%
P/NE:3	Pectin mixed with nanoemulsion of *trans*-cinnamaldehyde at the ratio of 3:1 (Pectin:NE)	2.50%
P/NE:4	Pectin imixed with nanoemulsion of *trans*-cinnamaldehyde at the ratio of 4:1 (Pectin:NE)	2.00%

2.4. Characterization of the Nanoemulsion

2.4.1. Size Distribution

The average particle size and size distributions of the emulsion droplets were determined by using dynamic light scattering (DLS) with a Zetasizer Nano-ZS90 instrument (Malvern Instruments Ltd., Worcestershire, UK) which is fixed at the angle of 90°. To eliminate multiple scattering effects and inter-droplet interactions, 1 mL of the nanoemulsion was diluted with 10 mL of distilled water, which served as a dispersant. After allowing for 90 s of equilibrium, the measurements were conducted in triplicate or more. The droplet size was described using the size average, while the polydispersity index (PDI) was used to assess the size distribution.

2.4.2. Zeta Potential (ζ)

The Zetasizer Nano-ZS90 instrument from Malvern Instruments Ltd., Worcestershire, UK, was used to determine the zeta potential. Electrophoretic mobility measurements were executed with disposable cuvettes. For sample preparation, 1 mL of nanoemulsion was combined with 10 mL of distilled water and thoroughly mixed. The Zeta potential measurements were performed in triplicate, and the resulting average value was computed.

2.5. Films Characterization

2.5.1. Film Thickness

An electronic micrometer (Walmart 0–25mm, 0.001mm) was used to determine the thickness of film samples. To calculate the average value, measurements were taken at a minimum of five random locations with an accuracy of 0.001 mm.

2.5.2. Opacity and Light Transmission of Films

The film sample was cut into rectangular strips (9 mm × 40 mm) and was placed in a spectrophotometer cell. Light transmission was measured at least three times at the wavelengths of 280 and 600 nm using a spectrophotometer (UV-3100pc, VMR, Miami, FL, USA). The empty spectrophotometer cell was used as the blank. Equation (1) was used to calculate the opacity of the films:

$$O = \frac{Abs\ 600}{thickness} \quad (1)$$

O (A × mm^{-1}) is film opacity and Abs 600 is absorbance at 600 nm.

2.5.3. Color Measurements

The colorimetric parameters of the films were evaluated using a colorimeter (Spectrophotometer CM-2300d, Konica Minolta, Tokyo, Japan). A standard white plate (L* = 92.34, a* = 1.03, b* = −1.65) was used as the background for color calibration. Chromaticity parameters including L* from black (0) to white (100), a* indicating red (+) to green (−) and b* indicating yellow (+) to blue (−) present in the sample were measured. At least five

points of each sample were selected to measure the color properties of the films. The total color differences (ΔE), whiteness (WI) and yellowness (YI) indexes were calculated for each sample according to Equations (2), (3), and (4), respectively [34].

$$\Delta E = \sqrt{(L^* - L)^2 + (a^* - a)^2 + (b^* - b)^2} \quad (2)$$

$$WI = 100 - \sqrt{(100 - L)^2 + a^2 + b^2} \quad (3)$$

$$YI = (142.86 \times b)/L \quad (4)$$

where L*, a* and b* are the color parameter values of the standard plate and L, a, and b are the color parameter values of the film samples.

2.5.4. Water Activity

The water activity of the film samples was measured using a Novasina water activity meter (Lab Swift-Aw Meter, Lachen, Switzerland) with an accuracy of ± 0.010 a_w. The film samples were cut into 2 × 2 cm and were analyzed in triplicate at an average room temperature of 23 ± 1 °C.

2.5.5. Mechanical Properties

Tensile strength (TS), elongation at break (%EB) and Young's modulus (YM) were measured according to the ASTM D882 standard method [35] using a tensile analyzer instrument (EZ-X Series, Shimadzu Company, Kyoto, Japan) with a 500 N load cell connected with an autograph software version 1.5.6 (Trapezium X, Shimadzu Corporation, Japan). Square film samples measuring 15 × 100 mm were prepared, and after conditioning at RH = 54% (saturated solution of Mg $(NO_3)_2$) for 48 h. The film samples were then placed between a pair of clamps with a gauge length of 50 mm each. The stretching occurred at a crosshead speed of 10 mm/min. The mechanical parameters were obtained from the force-deformation curves recorded using a computer using the given equations.

$$TS = \frac{\text{Force at break}}{\text{cross} - \text{sec tional area of specimenion}} \quad (5)$$

$$EB\ (\%) = \frac{\text{Change in length}}{\text{Initial film length}} \times 100 \quad (6)$$

$$YM = slope \times \frac{\text{Gauge lenght}}{cross - sectional\ area\ of\ specimen} \quad (7)$$

The cross-sectional area of the film was calculated using the width × the thickness.

2.5.6. Scanning Electron Microscopy

The study of the film structures was carried out using scanning electron microscopy (SEM) using an FEI Quanta 250 FEG microscope at the "Centre Technologique des Microstructures" (CTμ) at the University of Lyon in Villeurbanne, France. Film samples were applied to a flat steel holder and subjected to a vacuum coating process by cathodic sputtering prior to microscopic analysis. The sample was coated under vacuum by cathodic sputtering with 10 nm of copper before doing microscopy analysis and the analyze performed at working distance around 10 mm and energy beam of e10 kV.

2.5.7. Differential Scanning Calorimetry Analysis (DSC)

To determine the thermal parameters DSC analysis was performed associated with the endothermic peak areas on DSC thermograms. A Q 2000 DSC system (TA Instruments, New Castle, DE, USA) was used for this purpose. Film pieces weighing approximately 5 mg

were placed in a standard aluminum pan. The samples were subjected to a temperature increase ranging from −20 to 220 °C. The temperature increases constantly at a rate of 10 °C/min. During the analysis, the chamber was purged with nitrogen gas at a flow rate of 50 cm^3/min. The glass transition temperature (Tg) was determined using TA Universal Analysis Software [36] (https://www.tainstruments.com/).

2.5.8. Thermogravimetric Analysis (TGA)

Thermogravimetric analysis of the films was performed using a thermogravimetric analyzer instrument (TG 209, Netzsch Co., Selb, Germany). A total of 20 mg of each sample was precisely weighed in alumina crucibles. The temperature program involved a range from 20 °C to 600 °C, with a heating rate of 10 °C/min. All experiments were carried out in a nitrogen atmosphere at a flow rate of 20 mL/min. Weight loss was monitored in relation to temperature and time.

2.5.9. Attenuated Total Reflectance-Fourier-Transform Infrared (ATR-FTIR) Spectroscopy

The FTIR spectra of the pectin films were studied using an infrared (IR) spectrophotometer equipped with ATR (FTIR: Nicolet iS50, Thermo Scientific, Waltham, MA, USA) to investigate the interactions between pectin and *trans*-cinnamaldehyde within the films. FTIR spectra were recorded with a resolution of 4 cm^{-1} and 64 scans covering the spectral range 4000–400 cm^{-1}.

2.6. Evaluation of the Antimicrobial Activity of Films

The disk diffusion method was used to investigate the antibacterial effect of the films against Gram-positive bacteria, *Listeria innocua* (DSM20649) and Gram-negative bacteria, *Escherichia coli* (DSM613). The strains were stored at −20 °C in Tryptone Soy Broth (TSB) containing 15% (*v*/*v*) of glycerol. Bacteria were pre-cultured and diluted in TSB to obtain approximately 10^6 CFU/mL of each bacterium. One mL of pre-culture was used to inoculate the Petri dishes containing Tryptone Soy Agar plates (TSA) The film samples were cut into 16 mm diameter discs using a hole puncher in an aseptic manner. The disc of film was placed on the surface of TSA plates and then incubated at the temperature of 37 ± 1 °C for one day. The inhibition zone diameter around the discs was measured. For each film, experiments were performed in triplicate.

2.7. Statistical Analysis

The experiments were conducted at least three times, and the results are presented as the mean ± standard deviation for various samples. Statistical assessment involved one-way analysis of variance (ANOVA) followed by Fisher's test (F) to compare the means, and significance was determined at $p < 0.05$.

3. Results and Discussion

3.1. Particle Size and Zeta Potential of Nanoemulsion

After two stages of homogenization at high speed and high pressure, the mean particle size of the emulsions was 106 ± 2 nm. The polydispersity index (PDI) was also measured to provide information about the size distribution. The PDI was 0.24 ± 0.04, indicating the polydisperse distribution of oil droplets [37] in the emulsion according to ISO standards ISO 22412:2017 [38,39]. This small average size is due to the good emulsifying properties of lecithin, as it has a high affinity with the essential oil components [40]. Lecithin acts as a ripening inhibitor to prevent droplet growth. Ostwald ripening is a phenomenon that occurs in emulsions and nanoemulsions and results in larger droplets [37].

The average zeta potential was −57 ± 2 mV, indicating good emulsion stability due to the high zeta potential value. It is reported that a zeta potential value (negative or positive) of more than 30 mV represents a high degree of electrostatic repulsion and high resistance to aggregation, which causes stability in emulsions [41]. Lecithin is a negatively charged phospholipid that can be used to encapsulate insoluble or poorly soluble substances in

water with a good encapsulation rate [42]. This result is consistent with the measured zeta potential values, which ranged from −33.7 to −58.6 mV, obtained by changing the composition of emulsions prepared with 10% essential oils that were emulsified with 2% soybean lecithin and, as documented by [42].

3.2. Thickness, Opacity and Light Transmittance of Films

The addition of the nanoemulsion of TC influenced film thickness. The results are shown in Table 2. Higher concentrations of TC resulted in thinner films due to the reduction of the solid content. The film thickness varied between 63 and 91 µm from P/NE:1 to P/NE:4 ratios, while the thickness of pure pectin film was 102 µm.

Table 2. Physical properties of the film.

Sample Names	Thickness (µm)	Opacity (A × mm^{-1})	T 280 nm	T 600 nm	Water Activity
Pectin(control)	102 ± 2 ^{a}	0.73 ± 0.01 ^{e}	6.49 ± 0.89 ^{a}	83.83 ± 0.38 ^{a}	0.43 ± 0.01 ^{e}
P/NE:1	63 ± 1^{e}	1.42 ± 0.04 ^{c}	0 ^{b}	11.51 ± 0.82 ^{b}	0.58 ± 0.03 ^{a}
P/NE:2	72 ± 2 ^{d}	2.37 ± 0.07 ^{a}	0 ^{b}	2.15 ± 0.25 ^{e}	0.52 ± 0.02 ^{b}
P/NE:3	80 ± 2 ^{c}	1.67 ± 0.05 ^{b}	0 ^{b}	4.58 ± 0.50 ^{d}	0.52 ± 0.01 ^{c}
P/NE:4	91 ± 3 ^{b}	1.21 ± 0.03 ^{d}	0 ^{b}	7.93 ± 0.46 ^{c}	0.50 ± 0.04 ^{d}

The data are presented as the average ± one standard deviation (n = 3). Means that share identical letters show no significant differences ($p < 0.05$).

Transparency in food packaging is important because it influences the choices consumers make [43]. The higher the opacity value, the lower the transparency. Table 2 shows the opacity values of the films. The results showed that the opacity of the pectin films increased from 1.21 to 2.37 A × mm^{-1}, giving more opaque films compared to the neat pectin films with an opacity of 0.73 A × mm^{-1}. This is due to the dispersion of the nanoemulsion of TC into the film matrix. In fact, the scattering of lipid particles plays a role in coalescence, light-scattering, and creaming phenomena throughout the drying process. It caused the surface coarseness of the film and more opaque films [44]. A higher concentration of oil caused a higher value of opacity, except for P/NE:1 which can be explained by its thinner thickness and the very high concentration of TC (5%). The films with clove essential oil emulsions also showed a reduction in film opacity by adding essential oil emulsions [45].

The percentage of light transmittance at the wavelengths of 280 and 600 nm is shown in Table 2. The transmittance at a wavelength of 280 nm (UV range) was investigated to evaluate the UV barrier properties of the films. UV radiation can cause the oxidation of food products. Therefore, this parameter is an important factor when these films are used for food packaging in order to improve food preservation [46]. The addition of a TC nanoemulsion resulted in a complete UV barrier for pectin films. Pure pectin films had a transmittance of 6.49%, while all pectin films that incorporated a nanoemulsion of TC had a transmittance of zero percent at 280 nm.

Transmittance at a wavelength of 600 nm (visible range) was evaluated as a transparency factor and light transmission. A significant reduction was observed in transmittance at a wavelength of 600 nm with the addition of a TC nanoemulsion. The pure pectin films showed a high transmission of 83.83%, while the pectin film containing a nanoemulsion of TC had lower transmittances ranging between 11.51 and 2.15%.

The reduction in transmittance at both the 280 and 600 nm wavelengths could be attributed to the change in light absorption when combined with the nanoemulsion in the pectin film formulation and the effect of oil/lipid addition in the film matrix as well as the creation of irregularities that reduce specular light reflection [47]. The transmittance value of the samples at 600 nm was statistically different ($p < 0.05$) and followed the decreasing order P/NE:1 > P/NE:4 > P/NE:3 > P/NE:2. This tendency confirmed the reduction in light transmittance due to the presence of TC, except for P/NE:1. Surprisingly, P/NE:1

showed a higher transmittance compared to the other samples, which may be due to the thinner thickness and the high concentration of TC. The high concentration of TC may saturate the incorporation capacity of the pectin matrix, resulting in the presence of TC on the surface of the P/NE:1 film during the drying process. The reduction in transmittance by the addition of the nanoemulsion in the UV range (at 280 nm) is higher than in the visible range (at 600 nm). This suggests that the effect on the UV barrier properties of the film was more pronounced than the effect on the transparency of the film. This is worth noting because UV rays can cause oxidation and food spoilage. Thus, films with UV barrier properties can be considered suitable packaging that can extend the shelf life of foods [46]. The incorporation of rosemary oil into blended films based on carboxymethyl cellulose and polyvinyl alcohol also caused the reduction of transmittance at 280 and 600 nm wavelengths due to the inhibition of light transmission by nanoparticles as reported by [46].

3.3. Water Activity

Water activity is considered as a preservative factor in the food system [48]. The water activity (a_w) of the films was assessed in relation to the possibility of bacterial growth in the film. In fact, the a_w can indicate the microbiological stability of the films during the storage period when it is stored under humid conditions [49]. The a_w results are shown in Table 2. Most bacterial growth occurred with a_w ranging from 0.990 to 0.995, while some foodborne microorganisms, such as *Staphylococcus aureus*, can grow at an a_w of 0.860 [48].

The results of the a_w values ranged from 0.43 to 0.58 for pure pectin films and PNE 1 films and reflect the microbiological stability of all samples. The increase in a_w by the addition of a TC nanoemulsion was observed. This could be due to the hydrophobicity of TC. The same result was obtained for papaya edible films incorporating *Moringa oleifera* and ascorbic acid [49]. The a_w increased by incorporating antioxidant compounds with hydrophobic groups as reported by [50], who prepared edible films from native and phosphated cush-cush yam and cassava starch and reported water activity values from 0.47 to 0.52.

3.4. Color Measurements

The color parameters of pure pectin films and pectin films containing the nanoemulsified TC nanoemulsion are shown in Table 3. Except for the value of "L" and "a" for the film samples P/NE:2 and P/NE:3, the color parameters changed significantly by adding different concentrations of TC nanoemulsion. The incorporation of TC resulted in a yellowish color as can be seen in the image of the film samples in Figure 1.

Table 3. Color parameters of the films.

Sample Names	L	a	b	ΔE	WI	YI
Pectin (control)	90.22 ± 0.17 ^{a}	0.79 ± 0.19 ^{a}	4.48 ± 0.13 ^{e}	0.29 ± 0,02 ^{e}	89.12 ± 0.22 ^{a}	7.10 ± 0.31 ^{e}
P/NE:1	81.52 ± 0.61 ^{d}	−2.75 ± 0.28 ^{b}	55.11 ± 1.58 ^{a}	51.47 ± 1.54 ^{a}	41.79 ± 1.46 ^{e}	96.59 ± 2.65 ^{a}
P/NE:2	83.53 ± 0.84 ^{c}	−3.19 ± 0.30 ^{bc}	50.43 ± 1.38 ^{b}	46.44 ± 1.23 ^{b}	47.15 ± 1.06 ^{d}	85.17 ± 1.57 ^{b}
P/NE:3	84.58 ± 0.31 ^{c}	−3.78 ± 0.97 ^{c}	45.34 ± 4.21 ^{c}	41.64 ± 4.11 ^{c}	51.58 ± 3.88 ^{c}	77.54 ± 6.97 ^{c}
P/NE:4	87.29 ± 0.56 ^{b}	−4.88 ± 0.09 ^{d}	36.79 ± 1.89 ^{d}	32.91 ± 1.86 ^{d}	60.76 ± 1.81 ^{b}	60.21 ± 3.19 ^{d}

The data are presented as the average ± one standard deviation (n = 3). Means that share identical letters show no significant differences ($p < 0.05$).

The values of "L" and "a" indicate the lightness and redness of the film and both were reduced by the incorporation of the TC nanoemulsion. The values of "b" represent the yellowness, which increased significantly from the control to P/NE:1. A higher concentration of TC caused a higher value of "b" due to the native yellow color of TC, which is reflected by a high value of the YI (yellow index) for film samples containing TC compared to pure pectin films.

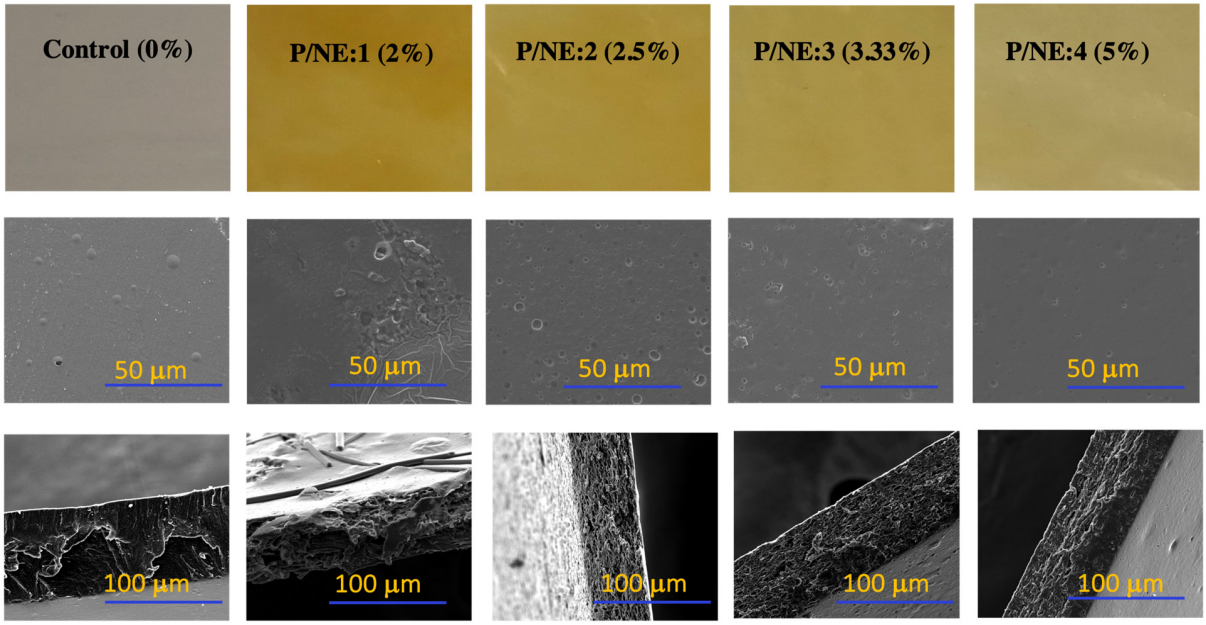

Figure 1. Visual aspect of film samples with different concentrations of *trans*-cinnamaldehyde: control (0%), P/NE:1 (5.00%), P/NE:2 (3.33%), P/NE:3 (2.50%) and, P/NE:4 (2.00%) (first line); microscopic images of the surface 1000× (SEM, middle line) and cross-sectional 800× (SEM, third line) of the pectin films with different contents of trans-cinnamaldehyde.

The color functions ΔE (degree of total color difference from the standard color plate), WI (whiteness index) and YI (yellow index) also changed significantly because of the integration of the nanoemulsion of TC into the film based on pectin. The value of ΔE extremely increased by the presence of TC. The value of ΔE was 51.47 for P/NE:1, while it was 0.29 for pure pectin. Higher concentrations of TC caused higher total color differences. The value of ΔE decreased by 36% from P/NE:1 to P/NE:4 by decreasing the concentration of oil from 5.00 to 2.00%. The same trend was observed for the YI value. This is due to the yellow color of TC; however, the control film was quite colorless, which is inconsistent with the film appearance as shown in Figure 1. The yellow color of TC changed the degree of whiteness (WI). A high reduction of WI was obtained in the range between 89.12 and 41.79 from pectin to P/NE:1. These changes in the color parameters could be attributed to light absorption as a consequence of the presence of TC and lipid [47].The same result was reported by [51], who incorporated various concentrations of TC in ethylene vinyl alcohol copolymer and observed an increase in YI value and ΔE value.

3.5. Mechanical Properties

The films proposed for food packaging applications must meet certain mechanical properties. Tensile strength (TS) is considered to be the highest stress the film can endure prior to breaking and percentage elongation to break (EB) provides information about the deformation of films before breakage while Young's modulus (YM) provides some information on the deformation before fracturing [52,53]. The mechanical characteristics of the films are shown in Table 4. The incorporation of TC into the film formulation significantly altered the mechanical parameters with statistical significance ($p < 0.05$). The pectin film without oil was mechanically more resistant to fracture with a TS value of 10.37 MPa, which was significantly decreased by adding TC nanoemulsion in the range of 67 to 12% from pectin film as a control to P/NE:1 and P/NE:4 ones, respectively.

Table 4. Mechanical properties of the films.

Samples	Tensile Strength (MPa)	Elongation at Break (%)	Young's Modulus (MPa)
Pectin (control)	10.37 ± 1.04 ^{a}	7.06 ± 0.42 ^{d}	317.59 ± 5.76 ^{a}
P/NE:1	3.32 ± 0.48 ^{d}	4.49 ± 0.53 ^{e}	100.65 ± 9.93 ^{d}
P/NE:2	5.10 ± 0.11 ^{c}	7.47 ± 0.22 ^{c}	126.90 ± 11.08 ^{cd}
P/NE:3	7.52 ± 0.21 ^{b}	8.62 ± 0,05 ^{b}	192.21 ± 18.37 ^{bc}
P/NE:4	9.03 ± 0.80 ^{ab}	8.77 ± 1.46 ^{a}	254.70 ± 19.80 ^{ab}

The data are presented as the average ± one standard deviation (n = 3). Means that share identical letters show no significant differences ($p < 0.05$).

The percentage of EB decreased for the highest TC concentration (5%) and increased for lower concentrations (2.0%, 2.5%, and 3.3%) compared to pectin films without TC. Another study also reported an increase in EB% by adding *Cinnamomum verum* into pectin films [54]. The presence of TC in the pectin film matrix resulted in a decrease not only in TS values, but also the elastic modulus. The incorporation of TC into the pectin film resulted in a decrease in Young's modulus values ranging from about 68 to 19% for TC concentrations ranging from 5.00 to 2.00%. The load parameters (TS and EB) were usually dependent on the microstructure film network and the intermolecular interactions [47,55]. The integration of TC into the film matrix results in softer films that are more prone to breaking and exhibit lower stretchability. This behavior could be due to the presence of structural discontinuities in the film network triggered by the lipid dispersed phase, leading to weak mechanical responses. Our results are in agreement with some previous studies showing a reduction in the tensile strength of polysaccharide films when a lipid is incorporated into the matrix of a biopolymer as reported By [56]. These authors incorporated different concentrations of bergamot, lemon, and tea tree essential oils into hydroxypropyl methylcellulose and chitosan, leading to significant reduction in the TS, EB% and elastic modulus of the films. In another study, chitosan-based films containing 0.5%, 1%, 2%, and 3% (*w*/*w*) bergamot essential oil showed lower resistance to break, lower deformable and lower tensile strength [55]. However, some studies reported an improvement in mechanical parameters in the presence of essential oils. The addition of clove oil into pectin films significantly increased the TS, YM, and EB% of the pectin films. This improvement was explained by the effect of chemical similarity between the clove oil particles and the pectin matrix, which favors a stronger interaction between the biopolymer matrix and dispersed particles [57]. Depending on the particular interactions between different types of polysaccharides and essential oils, the mechanical behavior varied according to different studies. It could be attributed to the effect of different materials and formulations and the use of various plasticizers and surfactants, temperature and relative humidity, etc. [55].

3.6. Scanning Electron Microscopy

Microscopy morphological analysis provides relevant information about the microstructure of pectin films and the effect of different TC concentrations in the film matrix. It provides a better understanding of the spatial arrangement of the film components, which can be used to study the mechanical properties and permeability of the films [58]. The visual aspect of the films as well as the scanning electron micrographs of the surface and cross sections of the pectin films are shown in Figure 1.

According to the cross-sectional micrographs, pure pectin presented a denser structure compared to films incorporated with TC nanoemulsion. In fact, the addition of oil droplets to the biopolymer matrix resulted in a sponge-like structure and increasing the TC concentration resulted in higher microcavities in the pectin film structure. However, continuous networks exhibited uniform dispersion of nanoemulsion, and oil droplets were homogenously entrapped in the biopolymer matrix. The pure pectin films had a smooth surface. The addition of 5.00% TC caused some roughness and irregularities on the surface

of the P/NE:1 sample. It could be due to the migration of the aggregates of droplets on the surface during the drying process for films containing high concentrations of TC. It is reported that flocculation and creaming of oil droplets could occur through the film drying process [56]. The other samples with lower concentration of TC, including P/NE:2, P/NE:3, and P/NE:4, represented the smoother surface. The surface images showed the presence of some pores on the surface of film samples. The samples containing TC had more pores compared to pure pectin films. The higher concentration of oil caused larger pore sizes, which can explain the coalescence phenomena for the oil droplet during drying as reported by [57]. A similar result was reported by [59,60] who developed a pectin-based film containing various concentrations of bioactive compounds. They observed the presence of pores or cavities by increasing the concentration of bioactive compounds.

3.7. ATR-FTIR Analysis

ATR-FTIR spectra were used to assess the intermolecular interactions and structural changes of the pectin film after the introduction of TC nanoemulsion. Figure 2 shows the ATR-FTIR spectra. The films exhibited broad absorption regions at approximately 3400 cm^{-1}, which are attributed to the stretching vibration of -OH bonds within the pectin monomers [61,62]. The peak appearing around 2927 cm^{-1} refers to -CH stretching vibration of methylene groups in pectin chains and methyl groups of methyl ester [61,63]. The peak at 1740 cm^{-1} corresponds to the C=O and C-O of ester bonds. It refers to the presence of the ester group formed by the esterification of pectin with a degree of esterification ranging from 22% to 28%. The vibrational peaks around 1670–1600 cm^{-1} and around 1400 cm^{-1} correspond to the asymmetric and symmetric vibrations of carboxyl groups, respectively [62,64]. The peak around 1010 cm^{-1} refers to C-O-C stretching vibrations of the polymer chain structure [65].

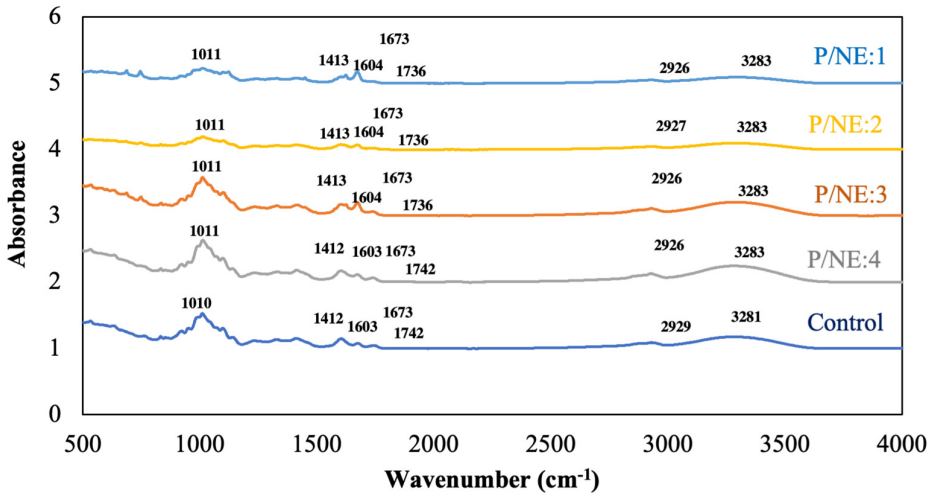

Figure 2. ATR-FTIR spectra of film samples with different concentrations of *trans*-cinnamaldehyde: Control (0%), P/NE:1 (5.00%), P/NE:2 (3.33%), P/NE:3 (2.50%) and, P/NE:4 (2.00%).

No new absorption peak was found in the pectin film spectra by adding the nanoemulsion of TC, indicating minor or no interactions between pectin and the nanoemulsion. Nevertheless, the O-H stretching vibration peak at approximately 3400 cm^{-1} underwent a slight shift from 3281 cm^{-1} to 3283 cm^{-1} upon the addition of TC. This could be caused by binding interactions between TC and pectin, which reduced the stretching of the free O-H bonds. The presence of TC also leads to changes in the band region around 2900 cm^{-1}, showing the shift of the band at 2929 cm^{-1} to 2926 cm^{-1}, which is related to the stretching vibration of the aliphatic C-H group (CH_2) [66]. The amplitude of the peak around 1740 cm^{-1} decreased slightly from the control sample to the film incorporated with nanoemulsion of TC. This peak corresponds to the C=O and C-O of ester bonds, which can be described by the presence of the carbonyl radical in the ester functional group of

triglycerides due to the presence of TC [66]. Similar results were reported by [57] who investigated the effect of incorporating different concentrations of clove bud essential oils into pectin films.

3.8. Thermogravimetric Analysis (TGA)

The thermal degradation and weight loss with temperature change in order to understand thermal tolerance of films were determined using TGA [60]. TGA curves can demonstrate the thermal stability of a material and its fraction of volatile components by monitoring the change in weight [67]. The thermogravimetry (TG) curves are shown in Figure 3, and the thermal data of film weight loss in the four intervals are also summarized in Table 5. All the films incorporated with the nanoemulsion of TC showed the same thermal behavior, similar to the neat pectin film. The mass change occurred in three steps. The first Is the region between 20 and 180 °C, which corresponds to the water evaporation associated with the hydrophilic groups in the polymeric structure [57] and the volatile part of TC. The loss mass of pure pectin was 9.05%. However, the P/NE:1 film containing 5.00% of TC lost 12.50% of its mass in the first step. This is probably due to the vaporization of the volatile component of TC.

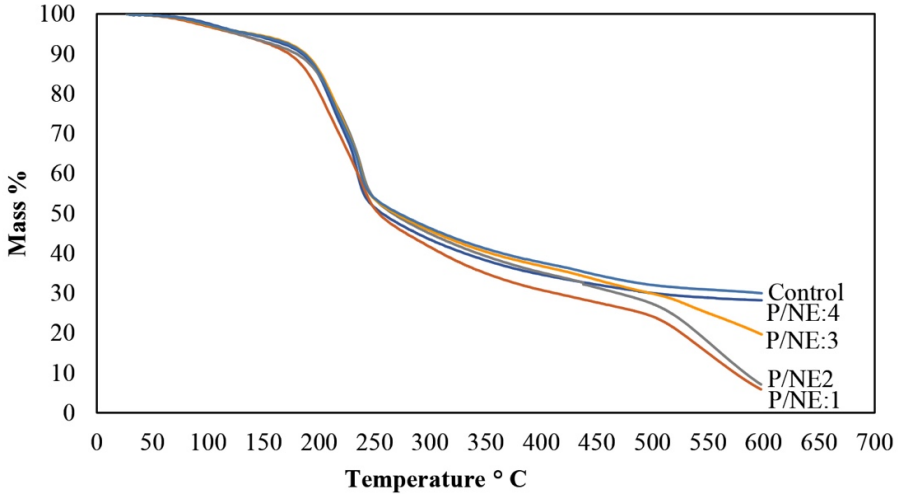

Figure 3. TGA thermogram of the control (pure pectin) and film samples based on pectin incorporated with different concentrations of 5.00%, 3.33%, 2.50%, and 2.00% *trans*-cinnamaldehyde incorporated in pectin film named P/NE:1, P/NE:2, P/NE:3, P/NE:4.

Table 5. Thermal parameters of the films.

	DSC	ATG (Δm)				DTG
Film Samples	**T_g °C**	**20–180 °C**	**180–260 °C**	**260–600 °C**	**20–600 °C**	**T_{max} °C Degradation**
Pectin (control)	152.94	9.05 ± 0.39 ^{b}	41.63 ± 1.23 ^{a}	19.67 ± 1.06 ^{c}	70.36 ± 0.22 ^{b}	234.83 ± 0.28 ^{b}
P/NE:1	13.72	12.50 ± 1.01 ^{a}	39.18 ± 0.62 ^{a}	41.65± 2.73 ^{a}	92.33 ± 1.10 ^{a}	239.16 ± 0.76 ^{a}
P/NE:2	40.90	10.71 ± 0.61 ^{ab}	39.25 ± 0.95 ^{a}	40.99 ± 4.17 ^{a}	91.95 ± 2.31 ^{a}	239 ± 1^{a}
P/NE:3	54	9.56 ± 0.59 ^{b}	39.07 ± 1.04 ^{a}	27.01 ± 3.66 ^{b}	75.64 ± 4.15 ^{b}	237 ± 0.30 ^{ab}
P/NE:4	57	9.45 ± 0.69 ^{b}	40.07 ± 1.37 ^{a}	21.52 ± 0.43 ^{bc}	71.14 ± 0.24 ^{b}	236 ± 0.43 ^{ab}

The data are presented as the mean ± one standard deviation (n = 3). Means that share identical letters show no significant differences ($p < 0.05$).

The main degradation of pure pectin sample occurred at the temperature of 180 to 260 °C, which is associated with decarboxylation of carbon ring and degradation of the polymer backbone [59,60]. There were no significant differences ($p < 0.05$) in the mass loss

of samples incorporated with TC and the pure pectin sample. The weight loss obtained ranged between 39.18 and 40.99% for samples ranging from pectin to P/NE:1.

The last part of the weight loss occurred at the higher temperature, which is explained by the formation of partially destroyed solid char stacks with a polyaromatic structure [68]. The final weight loss of the film incorporated with TC is higher than pure pectin film, due to the exitance of an aromatic structure in the *trans*-cinnamaldehyde. The higher concentration of TC in pectin films resulted in higher weight loss at high temperatures. Pure pectin lost 19.67% of its mass in this step, while the addition of 5.00% and 3.33% of TC caused a mass loss of 41.65 and 40.99% for P/NE:1 and P/NE:2, respectively. According to the results of mass loss with increasing temperature, the thermal stability of pectin films decreased by adding higher concentrations of TC (5.00% and 3.33%). However, the inclusion of 2.50% and 2.00% TC did not result in significant variations ($p < 0.05$) in initial mass loss compared to the pectin film control (containing 0% TC oil) within the temperature from 20 to 600 °C. The temperature at which the highest rate of weight loss occurred was obtained from the DTG thermogram named T_{max} °C degradation, which is shown in Table 5 for each sample. The same trend was observed by adding various concentrations of TC to pure pectin for the temperature of maximum weight loss rate. The presence of TC at concentrations of 5.00 and 3.33% caused an increase in this temperature compared to pure pectin. However, no significant differences were observed for the film containing 2.50 and 2.00% of TC compared to the pure pectin sample.

3.9. Differential Scanning Calorimetry (DSC)

The thermal properties of materials are investigated using DSC, a thermal analysis technique. It measures the heat flow into or out of a sample as a function of temperature or time. The DSC thermogram provides information about the phase transition of the sample. The structural changes caused by temperature variations were determined by using DSC for the film samples at temperature values between 20 and 220 °C. The glass transition temperature (Tg) is a phenomenon of amorphous polymers in which the transition from a glassy state to a rubber state occurs [69]. Tg was determined as an important factor for packaging material and the result is shown in Table 5. The packaging film can become soft at a temperature above Tg which could affect the packaging applications. The value of Tg significantly decreased by incorporating TC nanoemulsion. Tg was obtained at about 152.94 °C for pure pectin, while Tg was about 13.72 °C for P/NE:1, which is dramatically decreased as *trans*-cinnamaldehyde is hydrophobic. The decrease in Tg was reported by [70] who prepared an active film from ethylene vinyl alcohol copolymer incorporated with *trans*-cinnamaldehyde. The neat film exhibited a Tg of 55 °C, while the Tg value was 14 °C after the addition of TC.

3.10. Antimicrobial Activity

The diameter of the inhibition zones of the pectin film containing different concentrations of TC against *E. coli* and *L. innocua* is shown in Figure 4. The pure pectin film was considered as a control to investigate the potential antimicrobial activity of pure pectin. No inhibition zone appeared for pectin film without TC indicating no antimicrobial activity of the control. The diameters of the inhibition zones increased significantly by increasing the concentration of TC in the films for both bacteria tested. This is because more TC is available for release. Larger inhibition zone diameters were observed against *L. innocua,* a Gram-positive bacterium, compared to *E. coli*, a Gram-negative bacterium. The diameters of the inhibition zones varied from 37.41 to 30.46 mm for P/NE:1 to P/NE:4 for *L. innocua*. The same trend was obtained from 33.68 to 27.53 mm for P/NE:1 to P/NE:4 tested against *E. coli*. The presence of an extra hydrophilic membrane in Gram-negative bacteria hinders hydrophobic compound penetration like TC, leading to reduced inhibition zone diameters [71]. This result is consistent with the findings reported by [29], who incorporated a nanoemulsion of cinnamaldehyde into a pectin film. The larger diameters of the inhibition zones against *L.innocua* compared to *E.coli* were reported. It is reported

that enhancing the concentration of clove bud essential oil in pectin film led to greater antimicrobial activity [57]. Another study also reported the antimicrobial activity of pectin based films containing *Cinnamomum verum* against *Staphylococcus aureus (S. aureus), Listeria monocytogenes (L. monocytogenes), E. coli*, and *Salmonella typhimurium (S. typhimurium)* [71].

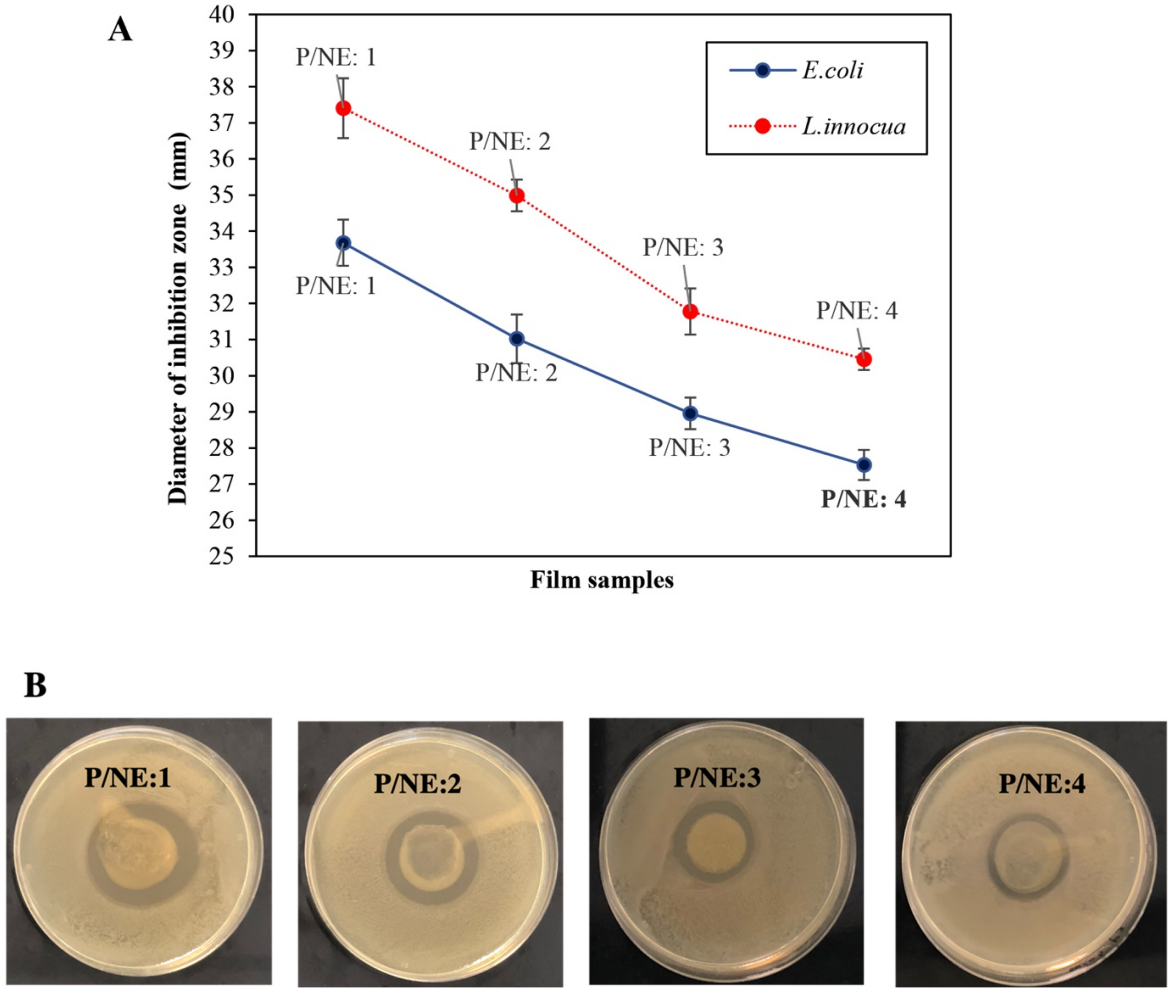

Figure 4. (**A**) Antimicrobial activity of pectin films containing a nanoemulsion of *trans*-cinnamaldehyde. (**B**) Diameters of the inhibition zones of *E. coli*; (images of inhibition zone on agar plates).

4. Conclusions

In this study, we examined the impacts of incorporating *trans*-cinnamaldehyde (TC) nanoemulsions into pectin for the development of antimicrobial food packaging films. Our results revealed significant impacts on the physical properties of the films. Emulsified pectin films exhibited increased opacity and improved light barrier properties. However, the presence of TC resulted in reduced tensile strength, elasticity, and elongation at break, especially at higher oil concentrations. Moreover, the addition of TC resulted in a reduction in thermal stability as confirmed by thermogravimetric analysis.

In order to evaluate the antimicrobial efficacy of the active films against foodborne bacteria, an agar disc-diffusion assay was carried out, which showed the presence of inhibition zones, and the antimicrobial activity was found to increase with increasing concentrations of TC. These findings indicate that pectin films containing TC nanoemulsions have potential for use in food preservation. However, further investigations are needed to evaluate the suitability of this packaging approach for different types of foodstuffs. Future studies should explore the specific application of these films in various food packaging scenarios to assess their effectiveness in real-world conditions. By expanding our understanding of

the potential applications of pectin-based films integrated with TC nanoemulsions, we can contribute to the development of advanced and efficient antimicrobial packaging materials for the food industry.

Author Contributions: Conceptualization, F.B., S.G. and A.G.; methodology, F.B.; validation, A.G., S.G. and E.D.; formal analysis, G.A.; investigation, A.G., S.G. and E.D.; writing—original draft, F.B.; writing—review and editing, S.G., E.D. and A.G.; supervision S.G., E.D. and A.G.; funding acquisition, S.G. All authors have read and agreed to the published version of the manuscript.

Funding: The authors express their gratitude to the TERRA ISARA foundation for providing financial support (grant number E-F0601-00) for this research project.

Data Availability Statement: The raw data supporting the conclusions of this article will be made available by the authors on request.

Conflicts of Interest: The authors declare no conflict of interest.

References

1. Chawla, R.; Sivakumar, S.; Kaur, H. Antimicrobial Edible Films in Food Packaging: Current Scenario and Recent Nanotechnological Advancements—A Review. *Carbohydr. Polym. Technol. Appl.* **2021**, *2*, 100024. [CrossRef]
2. Haghighi, H.; Gullo, M.; La China, S.; Pfeifer, F.; Siesler, H.W.; Licciardello, F.; Pulvirenti, A. Characterization of Bio-Nanocomposite Films Based on Gelatin/Polyvinyl Alcohol Blend Reinforced with Bacterial Cellulose Nanowhiskers for Food Packaging Applications. *Food Hydrocoll.* **2021**, *113*, 106454. [CrossRef]
3. Tambawala, H.; Batra, S.; Shirapure, Y.; More, A.P. Curcumin- A Bio-Based Precursor for Smart and Active Food Packaging Systems: A Review. *J. Polym. Environ.* **2022**, *30*, 2177–2208. [CrossRef]
4. Feig, V.R.; Tran, H.; Bao, Z. Biodegradable Polymeric Materials in Degradable Electronic Devices. *ACS Cent. Sci.* **2018**, *4*, 337–348. [CrossRef]
5. Yoo, S.-H.; Lee, B.-H.; Lee, H.; Lee, S.; Bae, I.Y.; Lee, H.G.; Fishman, M.L.; Chau, H.K.; Savary, B.J.; Hotchkiss, A.T. Structural Characteristics of Pumpkin Pectin Extracted by Microwave Heating. *J. Food Sci.* **2012**, *77*, C1169–C1173. [CrossRef] [PubMed]
6. Khalid, M.Y.; Arif, Z.U. Novel Biopolymer-Based Sustainable Composites for Food Packaging Applications: A Narrative Review. *Food Packag. Shelf Life* **2022**, *33*, 100892. [CrossRef]
7. Vinod, A.; Sanjay, M.R.; Suchart, S.; Jyotishkumar, P. Renewable and Sustainable Biobased Materials: An Assessment on Biofibers, Biofilms, Biopolymers and Biocomposites. *J. Clean. Prod.* **2020**, *258*, 120978. [CrossRef]
8. Meindrawan, B.; Suyatma, N.E.; Wardana, A.A.; Pamela, V.Y. Nanocomposite Coating Based on Carrageenan and ZnO Nanoparticles to Maintain the Storage Quality of Mango. *Food Packag. Shelf Life* **2018**, *18*, 140–146. [CrossRef]
9. Thomas, S.; Gopi, S.; Amalraj, A. *Biopolymers and Their Industrial Applications: From Plant, Animal, and Marine Sources, to Functional Products*; Elsevier: Amsterdam, The Netherlands, 2020; ISBN 978-0-12-819259-7.
10. Mellinas, C.; Ramos, M.; Jiménez, A.; Garrigós, M.C. Recent Trends in the Use of Pectin from Agro-Waste Residues as a Natural-Based Biopolymer for Food Packaging Applications. *Materials* **2020**, *13*, 673. [CrossRef]
11. Dranca, F.; Oroian, M. Extraction, Purification and Characterization of Pectin from Alternative Sources with Potential Technological Applications. *Food Res. Int.* **2018**, *113*, 327–350. [CrossRef]
12. Christiaens, S.; Uwibambe, D.; Uyttebroek, M.; Droogenbroeck, B.; van Loey, A.; Hendrickx, M. Pectin Characterisation in Vegetable Waste Streams: A Starting Point for Waste Valorisation in the Food Industry. *LWT Food Sci. Technol.* **2015**, *61*, 275–282. [CrossRef]
13. Roy, S.; Priyadarshi, R.; Łopusiewicz, Ł.; Biswas, D.; Chandel, V.; Rhim, J.-W. Recent Progress in Pectin Extraction, Characterization, and Pectin-Based Films for Active Food Packaging Applications: A Review. *Int. J. Biol. Macromol.* **2023**, *239*, 124248. [CrossRef]
14. Moslemi, M. Reviewing the Recent Advances in Application of Pectin for Technical and Health Promotion Purposes: From Laboratory to Market. *Carbohydr. Polym.* **2021**, *254*, 117324. [CrossRef]
15. Sánchez Aldana, D.; Andrade-Ochoa, S.; Aguilar, C.N.; Contreras-Esquivel, J.C.; Nevárez-Moorillón, G.V. Antibacterial Activity of Pectic-Based Edible Films Incorporated with Mexican Lime Essential Oil. *Food Control* **2015**, *50*, 907–912. [CrossRef]
16. Huang, J.; Hu, Z.; Hu, L.; Li, G.; Yao, Q.; Hu, Y. Pectin-Based Active Packaging: A Critical Review on Preparation, Physical Properties and Novel Application in Food Preservation. *Trends Food Sci. Technol.* **2021**, *118*, 167–178. [CrossRef]
17. Mungure, T.E.; Roohinejad, S.; Bekhit, A.E.-D.; Greiner, R.; Mallikarjunan, K. Potential Application of Pectin for the Stabilization of Nanoemulsions. *Curr. Opin. Food Sci.* **2018**, *19*, 72–76. [CrossRef]
18. Ravishankar, S.; Jaroni, D.; Zhu, L.; Olsen, C.; McHugh, T.; Friedman, M. Inactivation of Listeria Monocytogenes on Ham and Bologna Using Pectin-Based Apple, Carrot, and Hibiscus Edible Films Containing Carvacrol and Cinnamaldehyde. *J. Food Sci.* **2012**, *77*, M377–M382. [CrossRef] [PubMed]

19. Asdagh, A.; Pirsa, S. Bacterial and Oxidative Control of Local Butter with Smart/Active Film Based on Pectin/Nanoclay/Carum Copticum Essential Oils/β-Carotene. *Int. J. Biol. Macromol.* **2020**, *165*, 156–168. [CrossRef]
20. Nisar, T.; Yang, X.; Alim, A.; Iqbal, M.; Wang, Z.-C.; Guo, Y. Physicochemical Responses and Microbiological Changes of Bream (Megalobrama Ambycephala) to Pectin Based Coatings Enriched with Clove Essential Oil during Refrigeration. *Int. J. Biol. Macromol.* **2019**, *124*, 1156–1166. [CrossRef]
21. Chandrika, R.; Saraswathi, K.J.T.; Mallavarapu, G.R. Constituents of the Essential Oils of the Leaf and Root of *Eryngium foetidum* L. from Two Locations in India. *J. Essent. Oil Bear. Plants* **2015**, *18*, 349–358. [CrossRef]
22. Hyldgaard, M.; Mygind, T.; Meyer, R. Essential Oils in Food Preservation: Mode of Action, Synergies, and Interactions with Food Matrix Components. *Front. Microbiol.* **2012**, *3*, 12. [CrossRef]
23. Oussalah, M.; Caillet, S.; Saucier, L.; Lacroix, M. Inhibitory Effects of Selected Plant Essential Oils on the Growth of Four Pathogenic Bacteria: *E. coli* O157:H7, Salmonella Typhimurium, Staphylococcus Aureus and Listeria Monocytogenes. *Food Control* **2007**, *18*, 414–420. [CrossRef]
24. Johny, A.K.; Darre, M.J.; Hoagland, T.A.; Schreiber, D.T.; Donoghue, A.M.; Donoghue, D.J.; Venkitanarayanan, K. Antibacterial Effect of Trans-Cinnamaldehyde on Salmonella Enteritidis and Campylobacter Jejuni in Chicken Drinking Water. *J. Appl. Poult. Res.* **2008**, *17*, 490–497. [CrossRef]
25. CFR—Code of Federal Regulations Title 21. Available online: https://www.accessdata.fda.gov/scripts/cdrh/cfdocs/cfcfr/CFRSearch.cfm?fr=172.515&SearchTerm=cinnamaldehyde (accessed on 6 February 2024).
26. Friedman, M.; Henika, P.R.; Mandrell, R.E. Bactericidal Activities of Plant Essential Oils and Some of Their Isolated Constituents against *Campylobacter jejuni*, *Escherichia coli*, *Listeria monocytogenes*, and *Salmonella enterica*. *J. Food Prot.* **2002**, *65*, 1545–1560. [CrossRef]
27. Bowles, B.L.; Sackitey, S.K.; Williams, A.C. Inhibitory Effects of Flavor Compounds on *Staphylococcus aureus* Wrrc B1241. *J. Food Saf.* **1995**, *15*, 337–347. [CrossRef]
28. Almasi, H.; Azizi, S.; Amjadi, S. Development and Characterization of Pectin Films Activated by Nanoemulsion and Pickering Emulsion Stabilized Marjoram (*Origanum majorana* L.) Essential Oil. *Food Hydrocoll.* **2020**, *99*, 105338. [CrossRef]
29. Otoni, C.G.; de Moura, M.R.; Aouada, F.A.; Camilloto, G.P.; Cruz, R.S.; Lorevice, M.V.; de Soares, N.F.F.; Mattoso, L.H.C. Antimicrobial and Physical-Mechanical Properties of Pectin/Papaya Puree/Cinnamaldehyde Nanoemulsion Edible Composite Films. *Food Hydrocoll.* **2014**, *41*, 188–194. [CrossRef]
30. Pérez-Córdoba, L.J.; Norton, I.T.; Batchelor, H.K.; Gkatzionis, K.; Spyropoulos, F.; Sobral, P.J.A. Physico-Chemical, Antimicrobial and Antioxidant Properties of Gelatin-Chitosan Based Films Loaded with Nanoemulsions Encapsulating Active Compounds. *Food Hydrocoll.* **2018**, *79*, 544–559. [CrossRef]
31. Robledo, N.; Vera, P.; López, L.; Yazdani-Pedram, M.; Tapia, C.; Abugoch, L. Thymol Nanoemulsions Incorporated in Quinoa Protein/Chitosan Edible Films; Antifungal Effect in Cherry Tomatoes. *Food Chem.* **2018**, *246*, 211–219. [CrossRef]
32. Jantrawut, P.; Boonsermsukcharoen, K.; Thipnan, K.; Chaiwarit, T.; Hwang, K.-M.; Park, E.-S. Enhancement of Antibacterial Activity of Orange Oil in Pectin Thin Film by Microemulsion. *Nanomaterials* **2018**, *8*, 545. [CrossRef]
33. Norcino, L.B.; Mendes, J.F.; Natarelli, C.V.L.; Manrich, A.; Oliveira, J.E.; Mattoso, L.H.C. Pectin Films Loaded with Copaiba Oil Nanoemulsions for Potential Use as Bio-Based Active Packaging. *Food Hydrocoll.* **2020**, *106*, 105862. [CrossRef]
34. Tajik, S.; Maghsoudlou, Y.; Khodaiyan, F.; Jafari, S.M.; Ghasemlou, M.; Aalami, M. Soluble Soybean Polysaccharide: A New Carbohydrate to Make a Biodegradable Film for Sustainable Green Packaging. *Carbohydr. Polym.* **2013**, *97*, 817–824. [CrossRef] [PubMed]
35. Standard Test Method for Tensile Properties of Thin Plastic Sheeting. Available online: https://www.astm.org/d0882-18.html (accessed on 6 February 2024).
36. Battery Materials Lab Packages-TA Instruments. Available online: https://www.tainstruments.com/ (accessed on 13 February 2024).
37. Moghimi, R.; Ghaderi, L.; Rafati, H.; Aliahmadi, A.; McClements, D.J. Superior Antibacterial Activity of Nanoemulsion of Thymus Daenensis Essential Oil against *E. Coli*. *Food Chem.* **2016**, *194*, 410–415. [CrossRef] [PubMed]
38. Mudalige, T.; Qu, H.; Van Haute, D.; Ansar, S.M.; Paredes, A.; Ingle, T. Chapter 11—Characterization of Nanomaterials: Tools and Challenges. In *Nanomaterials for Food Applications*; López Rubio, A., Fabra Rovira, M.J., Martínez Sanz, M., Gómez-Mascaraque, L.G., Eds.; Micro and Nano Technologies; Elsevier: Amsterdam, The Netherlands, 2019; pp. 313–353, ISBN 978-0-12-814130-4.
39. *ISO 22412:2017*; Particle Size Analysis. Dynamic Light Scattering (DLS). ISO: Geneva, Switzerland, 2017. Available online: https://www.iso.org/standard/65410.html (accessed on 6 February 2024).
40. Donsì, F.; Annunziata, M.; Vincensi, M.; Ferrari, G. Design of Nanoemulsion-Based Delivery Systems of Natural Antimicrobials: Effect of the Emulsifier. *J. Biotechnol.* **2012**, *159*, 342–350. [CrossRef] [PubMed]
41. Duffy, J.; Larsson, M.; Hill, A. Suspension Stability; Why Particle Size, Zeta Potential and Rheology Are Important. *Annu. Trans. Nord. Rheol. Soc.* **2012**, *20*, 209–214.
42. Yang, Q.-Q.; Sui, Z.; Lu, W.; Corke, H. Soybean Lecithin-Stabilized Oil-in-Water (O/W) Emulsions Increase the Stability and In Vitro Bioaccessibility of Bioactive Nutrients. *Food Chem.* **2021**, *338*, 128071. [CrossRef] [PubMed]
43. Arrieta, M.P.; López, J.; Ferrándiz, S.; Peltzer, M.A. Characterization of PLA-Limonene Blends for Food Packaging Applications. *Polym. Test.* **2013**, *32*, 760–768. [CrossRef]

44. Ghanbarzadeh, B.; Almasi, H. Physical Properties of Edible Emulsified Films Based on Carboxymethyl Cellulose and Oleic Acid. *Int. J. Biol. Macromol.* **2011**, *48*, 44–49. [CrossRef] [PubMed]
45. Jahromi, M.; Niakousari, M.; Golmakani, M.T. Fabrication and Characterization of Pectin Films Incorporated with Clove Essential Oil Emulsions Stabilized by Modified Sodium Caseinate. *Food Packag. Shelf Life* **2022**, *32*, 100835. [CrossRef]
46. Fasihi, H.; Fazilati, M.; Hashemi, M.; Noshirvani, N. Novel Carboxymethyl Cellulose-Polyvinyl Alcohol Blend Films Stabilized by Pickering Emulsion Incorporation Method. *Carbohydr. Polym.* **2017**, *167*, 79–89. [CrossRef]
47. Atarés, L.; Bonilla, J.; Chiralt, A. Characterization of Sodium Caseinate-Based Edible Films Incorporated with Cinnamon or Ginger Essential Oils. *J. Food Eng.* **2010**, *100*, 678–687. [CrossRef]
48. Sperber, W.H. Influence of Water Activity on Foodborne Bacteria—A Review1. *J. Food Prot.* **1983**, *46*, 142–150. [CrossRef]
49. Rodríguez, G.M.; Sibaja, J.C.; Espitia, P.J.P.; Otoni, C.G. Antioxidant Active Packaging Based on Papaya Edible Films Incorporated with *Moringa oleifera* and Ascorbic Acid for Food Preservation. *Food Hydrocoll.* **2020**, *103*, 105630. [CrossRef]
50. Gutiérrez, T.J.; Morales, N.J.; Pérez, E.; Tapia, M.S.; Famá, L. Physico-Chemical Properties of Edible Films Derived from Native and Phosphated Cush-Cush Yam and *Cassava starches*. *Food Packag. Shelf Life* **2015**, *3*, 1–8. [CrossRef]
51. Aragón-Gutiérrez, A.; Heras-Mozos, R.; Gallur, M.; López, D.; Gavara, R.; Hernández-Muñoz, P. Hot-Melt-Extruded Active Films Prepared from EVOH/Trans-Cinnamaldehyde Blends Intended for Food Packaging Applications. *Foods* **2021**, *10*, 1591. [CrossRef] [PubMed]
52. Srinivasa, P.C.; Ramesh, M.N.; Tharanathan, R.N. Effect of Plasticizers and Fatty Acids on Mechanical and Permeability Characteristics of Chitosan Films. *Food Hydrocoll.* **2007**, *21*, 1113–1122. [CrossRef]
53. Ojagh, S.M.; Rezaei, M.; Razavi, S.H.; Hosseini, S.M.H. Development and Evaluation of a Novel Biodegradable Film Made from Chitosan and Cinnamon Essential Oil with Low Affinity toward Water. *Food Chem.* **2010**, *122*, 161–166. [CrossRef]
54. Khachani, R.; El Galiou, O.; Aitboulahsen, M.; Bakrim, H.; Arakrak, A.; Laglaoui, A.; Hassani Zerrouk, M. Stability of Antimicrobial, Antioxidant, and Functional Properties of Pectin-Based Film Incorporated with Thymus Capitatus and Cinnamomum Verum Essential Oils. *J. Food Saf.* **2024**, *44*, e13097. [CrossRef]
55. Sánchez-González, L.; Cháfer, M.; Chiralt, A.; González-Martínez, C. Physical Properties of Edible Chitosan Films Containing Bergamot Essential Oil and Their Inhibitory Action on Penicillium Italicum. *Carbohydr. Polym.* **2010**, *82*, 277–283. [CrossRef]
56. Sánchez-González, L.; Chiralt, A.; González-Martínez, C.; Cháfer, M. Effect of Essential Oils on Properties of Film Forming Emulsions and Films Based on Hydroxypropylmethylcellulose and Chitosan. *J. Food Eng.* **2011**, *105*, 246–253. [CrossRef]
57. Nisar, T.; Wang, Z.-C.; Yang, X.; Tian, Y.; Iqbal, M.; Guo, Y. Characterization of Citrus Pectin Films Integrated with Clove Bud Essential Oil: Physical, Thermal, Barrier, Antioxidant and Antibacterial Properties. *Int. J. Biol. Macromol.* **2018**, *106*, 670–680. [CrossRef]
58. Vargas, M.; Albors, A.; Chiralt, A.; González-Martínez, C. Characterization of Chitosan–Oleic Acid Composite Films. *Food Hydrocoll.* **2009**, *23*, 536–547. [CrossRef]
59. Shivangi, S.; Dorairaj, D.; Negi, P.S.; Shetty, N.P. Development and Characterisation of a Pectin-Based Edible Film That Contains Mulberry Leaf Extract and Its Bio-Active Components. *Food Hydrocoll.* **2021**, *121*, 107046. [CrossRef]
60. Lei, Y.; Wu, H.; Jiao, C.; Jiang, Y.; Liu, R.; Xiao, D.; Lu, J.; Zhang, Z.; Shen, G.; Li, S. Investigation of the Structural and Physical Properties, Antioxidant and Antimicrobial Activity of Pectin-Konjac Glucomannan Composite Edible Films Incorporated with Tea Polyphenol. *Food Hydrocoll.* **2019**, *94*, 128–135. [CrossRef]
61. Pasini Cabello, S.D.; Takara, E.A.; Marchese, J.; Ochoa, N.A. Influence of Plasticizers in Pectin Films: Microstructural Changes. *Mater. Chem. Phys.* **2015**, *162*, 491–497. [CrossRef]
62. Wathoni, N.; Yuan Shan, C.; Yi Shan, W.; Rostinawati, T.; Indradi, R.B.; Pratiwi, R.; Muchtaridi, M. Characterization and Antioxidant Activity of Pectin from Indonesian Mangosteen (*Garcinia mangostana* L.) Rind. *Heliyon* **2019**, *5*, e02299. [CrossRef] [PubMed]
63. Roy, S.; Rhim, J.-W. Preparation of Pectin/Agar-Based Functional Films Integrated with Zinc Sulfide Nano Petals for Active Packaging Applications. *Colloids Surf. B Biointerfaces* **2021**, *207*, 111999. [CrossRef] [PubMed]
64. Manrique, G.D.; Lajolo, F.M. FT-IR Spectroscopy as a Tool for Measuring Degree of Methyl Esterification in Pectins Isolated from Ripening Papaya Fruit. *Postharvest Biol. Technol.* **2002**, *25*, 99–107. [CrossRef]
65. Gnanasambandam, R.; Proctor, A. Determination of Pectin Degree of Esterification by Diffuse Reflectance Fourier Transform Infrared Spectroscopy. *Food Chem.* **2000**, *68*, 327–332. [CrossRef]
66. Vlachos, N.; Skopelitis, Y.; Psaroudaki, M.; Konstantinidou, V.; Chatzilazarou, A.; Tegou, E. Applications of Fourier Transform-Infrared Spectroscopy to Edible Oils. *Anal. Chim. Acta* **2006**, *573–574*, 459–465. [CrossRef] [PubMed]
67. Rajisha, K.R.; Deepa, B.; Pothan, L.A.; Thomas, S. 9—Thermomechanical and Spectroscopic Characterization of Natural Fibre Composites. In *Interface Engineering of Natural Fibre Composites for Maximum Performance*; Zafeiropoulos, N.E., Ed.; Woodhead Publishing Series in Composites Science and Engineering; Woodhead Publishing: Sawston, UK, 2011; pp. 241–274, ISBN 978-1-84569-742-6.
68. Wang, W.; Ma, X.; Jiang, P.; Hu, L.; Zhi, Z.; Chen, J.; Ding, T.; Ye, X.; Liu, D. Characterization of Pectin from Grapefruit Peel: A Comparison of Ultrasound-Assisted and Conventional Heating Extractions. *Food Hydrocoll.* **2016**, *61*, 730–739. [CrossRef]
69. Ahmad, M.M.; Chauhan, K.; Naz, A.; Nayeem, M. Antimicrobial and Antioxidant Activity of Impregnated Pectin and Alginate Based Bio Composite Packaging Material for Fresh Produce Safety. *Pharma Innov.* **2021**, *10*, 262–272. [CrossRef]

70. Gurunathan, S. Biologically Synthesized Silver Nanoparticles Enhances Antibiotic Activity against Gram-Negative Bacteria. *J. Ind. Eng. Chem.* **2015**, *29*, 217–226. [CrossRef]
71. Fisher, K.; Phillips, C.A. The Effect of Lemon, Orange and Bergamot Essential Oils and Their Components on the Survival of *Campylobacter jejuni*, *Escherichia coli* O157, *Listeria monocytogenes*, *Bacillus cereus* and *Staphylococcus aureus* in Vitro and in Food Systems. *J. Appl. Microbiol.* **2006**, *101*, 1232–1240. [CrossRef] [PubMed]